JOURNAL OF MATERIALS SCIENCE **37** (2002) 2983–2987

Interlaminar fracture characterization for plain weave fabric composites

N. K. NAIK, K. S. REDDY, S. MEDURI, N. B. RAJU, P. D. PRASAD, SK. N. M. AZAD, P. A. OGDE, B. C. K. REDDY
Aerospace Engineering Department, Indian Institute of Technology-Bombay, Powai, Mumbai -400 076, India
E-mail: nknaik@aero.iitb.ac.in

For the analysis of laminated composite plates under transverse loading and drilling of composites, all the elastic, strength and fracture properties of the composite plates are essential. Interlaminar critical strain energy release rate properties in mode I, mode II, mixed mode I/II and mode III have been evaluated for two types of plain weave fabric *E*-glass/epoxy laminates. The double cantilever beam test and the end notch flexure test have been used for mode I and mode II loading. The mixed mode bending test and split cantilever beam test have been used for mixed mode I/II and mode III loading. It is observed that the plain weave fabric composite with lesser strand width has higher interlaminar fracture properties compared to the plain weave fabric composite with more strand width. Further, crack length versus crack growth resistance plots have been presented for mode III loading. In general, it is observed that total fracture resistance is significantly higher than the critical strain energy release rate.

Nomenclature

a	=	Initial crack length
a_f, a_w	=	Strand width
b	=	Width of the specimen
c	=	Loading lever length for mixed mode I/II testing
E_{11}	=	Young's modulus of the specimen along the span length
g_f, g_w	=	Inter-strand gap
G_{IC}, G_{IIC}, G_{IIIC}	=	Mode I, mode II, mode III interlaminar critical strain energy release rates
G_{IRC}, G_{IIRC}, G_{IIIRC}	=	Mode I, mode II, mode III total fracture resistance
G_{TC}	=	Mixed mode I/II interlaminar critical strain energy release rate
G_{TRC}	=	Mixed mode I/II total fracture resistance
h	=	Half the thickness of the specimen
h_f, h_w	=	Strand thickness
h_t	=	Fabric thickness
h_m	=	Thickness of matrix
H_L	=	Lamina thickness
L	=	Specimen half span
P	=	Applied load
P_I, P_{II}	=	Mode I and mode II components of the load for mixed mode I/II testing
P_{IC}	=	Applied critical load for mode I testing
P_{IIC}	=	Applied critical load for mode II testing
δ	=	Crack opening displacement

1. Introduction

Delamination between the adjacent layers is a fundamental mode of failure in laminated composites. Such delaminations initiate and propagate under the influence of normal and shear stresses. For the effective use of composites, delamination resistance characteristics are the important considerations. Delamination initiation and propagation for a given loading condition mainly depends upon the interlaminar critical strain energy release rate (G_c). The delamination propagation can be in mode I, mode II, mixed mode I/II or mode III loading conditions. Considering the importance of this subject there are many studies on the determination of G_c under different loading conditions [1–14]. For typical loading conditions such as transverse loading and drilling of laminated composites, interlaminar critical strain energy release rate properties in mode I, mode II, mixed mode I/II and mode III are essential.

Traditionally, laminated composites made of unidirectional (UD) prepegs are used for high in-plane specific strength and high in-plane specific stiffness applications. But such materials have lower interlaminar fracture properties. One of the ways to enhance the interlaminar fracture properties is to make use of woven fabric (WF) composites for structural applications. It may be noted that WF composites have relatively lower in-plane elastic and strength properties.

For the characterization of behaviour of laminated composites under transverse loading the interlaminar fracture properties in mode I, mode II, mixed mode I/II and mode III are essential. It was observed from the literature that all these properties are not readily available for the same material. The objective of the present

work is to determine all these interlaminar fracture properties for the same material. The double cantilever beam (DCB) test and end notch flexure (ENF) test [1, 14] have been used for mode I and mode II loading. The mixed mode bending (MMB) test [4, 7, 11] and the split cantilever beam (SCB) test [2, 3, 5] have been used for mixed mode I/II and the mode III loading.

Thermomechanical and fracture properties of WF composites depend upon the weave pattern such as plain, twill and satin and the fabric geometry. In the present study, interlaminar critical strain energy release rate properties have been evaluated for two types of plain weave fabric E-glass/epoxy laminates. Effect of fabric geometry on the interlaminar fracture properties has also been studied.

A general plain weave fabric lamina geometrical representative unit cell is shown in Fig. 1. A photomicrograph of a typical plain weave fabric laminate cross-section is shown in Fig. 2. The plain weave fabric is produced by interlacing the warp and fill strands in a regular sequence of one under and one over. The strand width, strand thickness and inter-strand gap are the main geometrical parameters. The suffixes w and f refer to warp and fill.

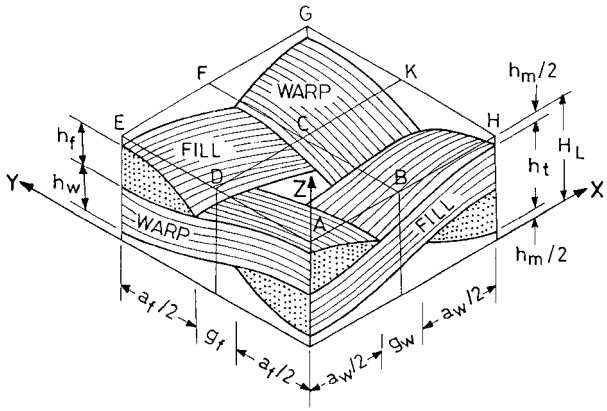

Figure 1 Plain weave fabric lamina geometrical representative unit cell.

2. Theory

Schematic arrangements of the specimens for different modes of loading are given in Fig. 3. Interlaminar critical strain energy release rates are calculated as follows: Using the DCB test [1, 14]

$$G_{IC} = \frac{12a^2 P_{IC}^2}{b^2 h^3 E_{11}} \tag{1}$$

Using the ENF test [1, 14]

$$G_{IIC} = \frac{9a^2 P_{IIC}^2}{16b^2 h^3 E_{11}} \tag{2}$$

Using the MMB test [4]

$$G_{TC} = G_I + G_{II} \tag{3}$$

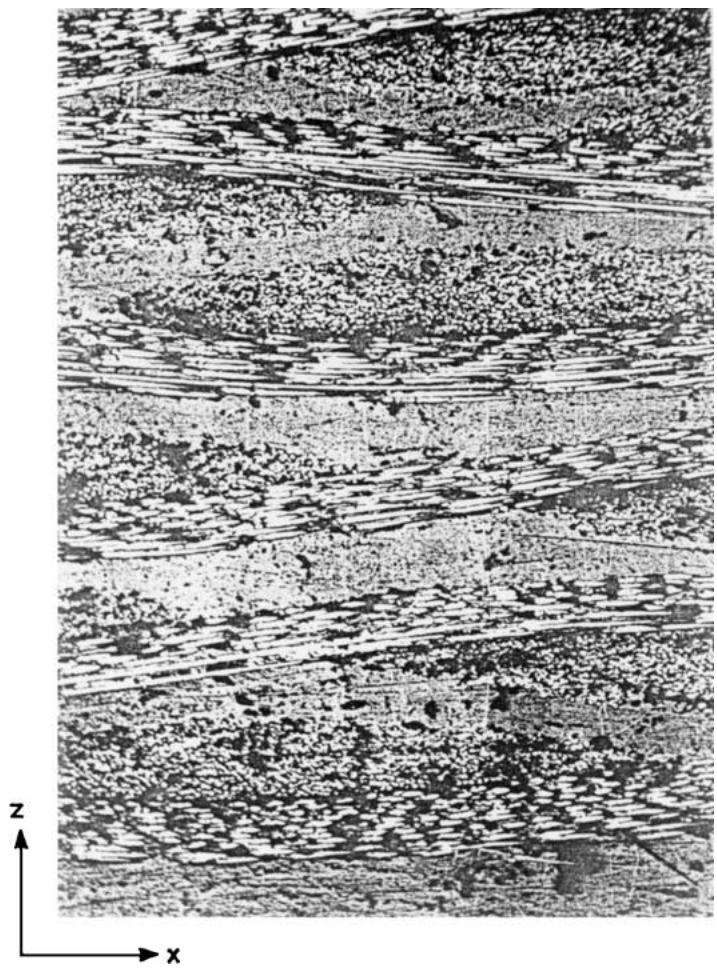

Figure 2 Photomicrograph of a typical plain weave fabric laminate cross-section.

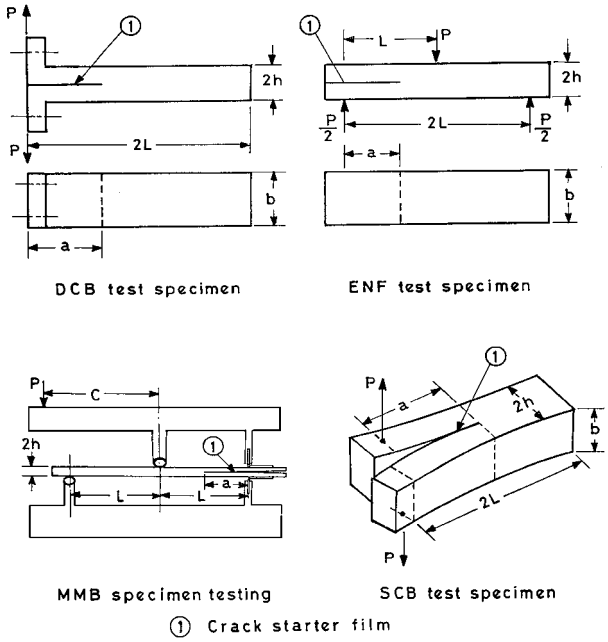

Figure 3 Geometry and loading for interlaminar fracture testing.

$$G_{\mathrm{I}} = \frac{12a^2P_{\mathrm{I}}^2}{b^2h^3E_{11}} \tag{4}$$

where

$$P_{\mathrm{I}} = \left(\frac{3c - L}{4L}\right)P$$

$$G_{\mathrm{II}} = \frac{9a^2P_{\mathrm{II}}^2}{16b^2h^3E_{11}} \tag{5}$$

where

$$P_{\mathrm{II}} = \left(\frac{c + L}{L}\right)P$$

Using the SCB test [2, 3]

$$G_{\mathrm{III}} = \frac{1}{2b}\left[P\,\frac{\mathrm{d}\delta}{\mathrm{d}a} - \delta\frac{\mathrm{d}P}{\mathrm{d}a}\right] \tag{6}$$

3. Test details

The DCB test was used for mode I fracture characterization. The specimen thicknesses were derived based on the small deflection linear elastic load-displacement response [15]. Specimen dimensions were: $h = 4$ mm, specimen length, $2L = 140$ mm, $b = 25$ mm, $a = 25$ mm.

The ENF test was used for mode II fracture characterization. Specimen dimensions were: $h = 4$ mm, $b = 25$ mm, $L = 50$ mm, $a = 25$ mm.

The MMB test was used for mixed mode I/II fracture characterization. Specimen dimensions were: $h = 4$ mm, $b = 25$ mm, $L = 50$ mm, $a = 25$ mm, loading lever length, $c = 63$ mm.

The SCB test was used for mode III fracture characterization. Specimen dimensions were: cross-sectional area $(2h \times b) = 25$ mm $\times$ 25 mm, specimen length, $2L = 280$ mm, $a = 50$ mm.

All the interlaminar fracture tests have been carried out on two types of plain weave fabric E-glass/epoxy laminates, GLE-12 and GLE-13. The fibre volume fraction (V_{f}°) for GLE-12 and GLE-13 was 0.44 and 0.40, respectively. The fabric geometry is presented in Table I. Interlaminar fracture properties have been obtained with respect to warp direction and at 45° orientation with respect to warp direction.

4. Data reduction

During testing, crack propagation as a function of applied load was noted. Crack length versus applied load data has been obtained for all the loading cases. For mode III test, crack length versus crack opening displacement data has also been obtained. Crack length versus applied load and crack opening displacement plots have been presented in Fig. 4 for GLE-12 specimens under mode III loading. A polynomial curve fit of order 6 has been used. Using the local slope of these curves and corresponding crack length, crack growth resistance curves, i.e., crack length versus G_{c} plots have been obtained for mode III loading case (Fig. 5). Similar data has been derived for mode I, mode II and mixed mode I/II loading cases also. Critical strain energy release rate (G_{c}) and total fracture resistance (G_{RC}) values have been presented in Tables II and III, respectively for both GLE-12 and GLE-13. The properties

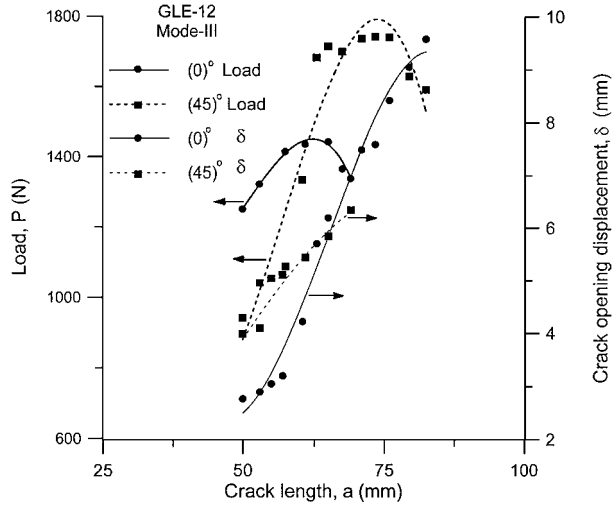

Figure 4 Load and crack opening displacement as a function of crack length for E-glass/epoxy laminates, WF, GLE-12 : Mode-III.

TABLE I Plain weave fabric geometry

Material	Fabric thickness, h_{t} (mm)	Fill strand: Strand count (per cm)	Fill strand: a_{f} (mm)	Fill strand: h_{f} (mm)	Fill strand: g_{f} (mm)	Warp strand: Strand count (per cm)	Warp strand: a_{w} (mm)	Warp strand: h_{w} (mm)	Warp strand: g_{w} (mm)	V_{f}°
GLE-12	0.26	5.40	1.75	0.13	0.10	5.90	1.60	0.13	0.07	0.44
GLE-13	0.62	2.30	3.75	0.31	0.59	2.80	3.15	0.31	0.42	0.40

TABLE II Interlaminar critical strain energy release rate (J/m^2)

	G_{IC}		G_{IIC}		G_{TC}		G_{IIIC}	
Material	0°	45°	0°	45°	0°	45°	0°	45°
GLE-12	387 (±10)	260 (±18)	1343 (±59)	1168 (±11)	850 (±59)	558 (±32)	2767 (±85)	751 (±12)
GLE-13	212 (±59)	186 (±85)	1022 (±74)	1369 (±92)	265 (±2)	232 (±14)	1919 (±281)	269 (±44)

TABLE III Interlaminar total fracture resistance (J/m^2)

	G_{IRC}		G_{IIRC}		G_{TRC}		G_{IIIRC}	
Material	0°	45°	0°	45°	0°	45°	0°	45°
GLE-12	1063 (±286)	331 (±89)	2648 (±582)	6469 (±1799)	850 (±59)	558 (±32)	3250 (±715)	9055 (±738)
GLE-13	445 (±159)	429 (±81)	3642 (±5)	1835 (±41)	679 (±66)	265 (±116)	6134 (±304)	5668 (±1835)

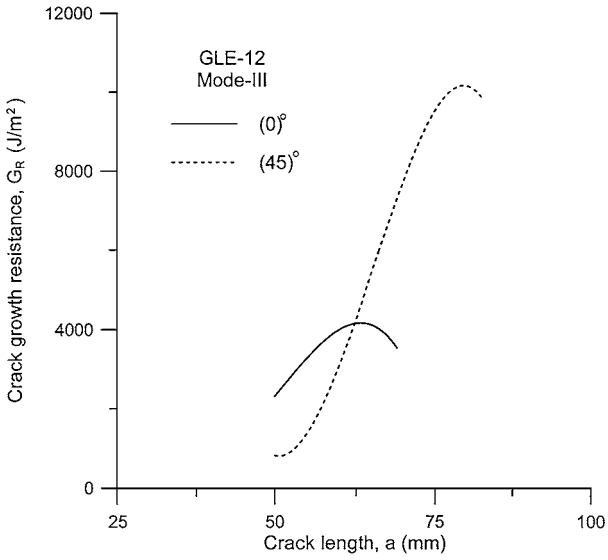

Figure 5 Crack growth resistance as a function of crack length for *E*-glass/epoxy laminates, WF, GLE-12 : Mode-III.

have been obtained along warp direction referred to as 0° direction. Also, the properties have been obtained at 45° direction with respect to the warp direction.

Crack length versus load plots can be subdivided into three regions. In the first region, i.e., upto a critical applied load, there would not be any crack propagation as the load is increased. The load at which the crack just starts propagating is the critical load and the corresponding strain energy release rate is the critical strain energy release rate. This particular point is the second region. Beyond this critical load, there would be more resistance for further crack propagation. This indicates total fracture resistance (G_{TR}). This is shown in Fig. 5 for mode III loading case. The corresponding region is the third region. Such plots are also called *R*-curves. Here, G_{TR} increases as the crack length increases reaching to a plateau. The corresponding crack length refers to the limiting case of stable crack growth. The corresponding value is indicated as G_{TRC}. The possible reasons for *R*-curve effect, i.e., the increase in resistance for further crack growth are: strand/fibre wandering from one layer to the adjacent layer, curvilinear path of the interfaces for the WF composites and the interpenetration of the strands of one layer into the adjacent layers during consolidation.

5. Results and discussion

A WF laminate is formed by stacking WF layers one over the other. For actual fabrics, the distribution of strands of one layer is not in exact alignment with the distribution of strands of the adjacent layers. The strands of one layer can be shifted along the warp, fill and/or thickness direction with respect to strands of the adjacent layers. In an actual laminate, the relative movements of the fabric layers are affected by friction between fabric layers, local departure in strand perpendicularity, possible variation of strand count from place to place in the fabric and constraints on the relative lateral movement of the layer, during lamination. Hence, an actual WF laminate would have scattered zones of different combinations of shifts as shown in Fig. 2. With this, the interlaminar properties may vary from sample to sample. This is the possible reason for a wide scatter in interlaminar fracture properties as shown in Tables II and III. The properties presented are the averages of four test results.

From Tables II and III, in general, it can be seen that $G_{IC} < G_{TC} < G_{IIC} < G_{IIIC}$ for both 0° and 45° orientations. Also, it can be seen that G_c with respect to 45° orientation is less than G_c with respect to 0° orientation. The scatter is more for G_{RC} than for G_c.

For GLE-12, fill strand width is 1.75 mm and warp strand width is 1.60 mm. For GLE-13, fill strand width is 3.75 mm and warp strand width is 3.15 mm. If the width of the strand is less, the deviation from the linear path of the crack front would be more. This would lead to more resistance for crack propagation. Hence, GLE-12 has higher interlaminar fracture properties compared to those for GLE-13.

For the analysis of laminated composite plates under transverse static/impact loading, material elastic, strength and interlaminar fracture properties are necessary. In our earlier studies all the elastic and strength properties for plain weave fabric *E*-glass/epoxy laminate GLE-12 have been presented [16]. As a part of the present work interlaminar fracture properties in mode I, mode II, mixed mode I/II and mode III have been presented. With these properties structural analysis of

laminated composites made of GLE-12 under certain loading conditions can be taken up.

6. Conclusions

1. In general, it is observed that $G_{IC} < G_{TC} < G_{IIC} < G_{IIIC}$.

2. G_c with respect to 45°orientation is less than G_c with respect to 0° orientation.

3. The plain weave fabric composite with lesser strand width has higher interlaminar fracture properties compared to the plain weave fabric composite with more strand width.

Acknowledgements

This work was supported by the Structures Panel, Aeronautics Research & Development Board, Ministry of Defence, Government of India, Grant No. Aero/RD-134/100/10/95-96/890.

References

1. J. M. WHITNEY, I. M. DANIEL and R. B. PIPES, in "Experimental Mechanics of Fiber Reinforced Compoiste Materials" (The Society for Experimental Mechanics, Brookfield Center, Connecticut, 1984) p. 233.
2. S. L. DONALDSON, *Composites Science and Technology* **32** (1988) 225.
3. S. L. DONALDSON and S. MALL, *Journal of Reinforced Plastics and Composites* **8** (1989) 91.
4. J. R. REEDER and J. H. CREWS, JR., *AIAA Journal* **28** (1990) 1270.
5. S. L. DONALDSON, S. MALL and C. LINGG, *Journal of Composites Technology and Research* **13** (1991) 41.
6. P. ROBINSON and D. Q. SONG, *Composites Science and Technology* **52** (1994) 217.
7. M. L. BENZEGGAGH and M. KENANE, *ibid.* **56** (1996) 439.
8. J. LI and T. K. O'BRIEN, *Journal of Composites Technology and Research* **18** (1996) 96.
9. W. C. LIAO and C. T. SUN, *Composites Science and Technology* **56** (1996) 489.
10. N. ALIF, L. A. CARLSSON and L. BOOGH, *Composites* B **29B** (1998) 603.
11. K. N. SHIVA KUMAR, J. H. CREWS, JR. and V. S. AVVA, *Journal of Composite Materials* **32** (1998) 804.
12. A. P. MOURITZ, C. BAINI and I. HERSZBERG, *Composites* A **30A** (1999) 859.
13. N. K. NAIK, N. BULLI RAJU, P. DURGA PRASAD, SAILENDRA MEDURI, SK. N. M. AZAD, K. SATYANARAYANA REDDY and P. A. OGDE, in Proceeding of ICEM-IX (Society for Experimental Mechanics, Inc., Bethal, Connecticut, 2000) p. 754.
14. E. E. GDOUTS, K. PILAKOUTAS and C. A. RODOPOULOS, in "Failure Analysis of Industrial Composite Materials" (McGraw-Hill, New York, 2000) p. 147.
15. J. W. GILLESPIE, JR. and L. A. CARLSSON, in "Delaware Composites Design Encyclopedia," Vol. 6 (Techromic Publishing Co., Inc., Lancaster, 1990) p. 113.
16. N. K. NAIK, Y. CHANDRA SEKHER and M. SAILENDRA, *Journal of Reinforced Plastics and Composites* **19** (2000) 912.

Received 17 May 2001
and accepted 14 February 2002